Tikrit Journal of Engineering Sciences (2025); 32(4): 2108
DOI: http://doi.org/10.25130/tjes.32.4.4

IRAQI Academic Scientific Journals

ISSN: 1813-162X (Print); 2312-7589 (Online)

Tikrit Journal of Engineering Sciences

available online at: http://www.tj-es.com

TJES Tikrit Journal of Engineering Sciences

The Effect of Co-Surfactant Charge on the Structure Properties of Prepared Nano SBA-15 Using Sodium Silicate

Yousra S. Kareem *[a,b], Hussein Q. Hussein [b]

[a] Chemical Department, Engineering College, Baghdad University, Baghdad, Iraq.
[b] Chemical Department, Engineering College, Al-Nahrain University, Baghdad, Iraq.

Keywords:
CTAB; Co-Surfactants; F68; p123 micelles; SBDS; SBA-15; Sodium Silicate.

Highlights:

- Pure mesoporous SBA-15 with three different charges.
- Study the effect of co-surfactants on particle dispersion, texture properties, and morphologies.
- Using a new co-surfactant (SBDS).

ARTICLE INFO

Article history:

Received	29 Mar. 2024
Received in revised form	23 May 2024
Accepted	26 Sep. 2024
Final Proofreading	22 Aug. 2025
Available online	29 Aug. 2025

Citation: Kareem YS, Hussein HQ. **The Effect of Co-Surfactant Charge on the Structure Properties of Prepared Nano SBA-15 Using Sodium Silicate**. *Tikrit Journal of Engineering Sciences* 2025; **32**(4): 2108.
http://doi.org/10.25130/tjes.32.4.4

*Corresponding author:
Yousra S. Kareem
Chemical Department, Engineering College, Baghdad University, Baghdad, Iraq.

Abstract: Mesoporous SBA-15 with nono particle size distribution, different texture properties, and morphologies have been synthesized by controlling the hydrophilic-hydrophobic character during preparation, i.e., the solubility of micelles of pluronic P123 by controlling the charge of PEO hydrophilic-inorganic silica zone using different charge surfactants CTAB (cationic), F68 (nonionic), and SDBS (anionic). Sodium silicate was used as a silica source. $Eo_{20}Po_{70}Eo_{20}$ co-polymer was used as a template at highly acidic conditions (pH<2). The experiments were characterized using XRD, FTIR, AFM, BET, and FESEM. The XRD and FTIR tests indicated that the SBA-15 is amorphous and free from impurities. The degree of particle dispersion is sequenced according to the order CTAB> SBDS> F68> bare p123. Also, the texture properties were between (577-900) m^2/g surface area, (0.28-0.47) cm^3/g pore volume and (1.98-2.3) nm pore size. The optimum texture properties were achieved using CTAB co-surfactant.

دراسة تاثير شحنة المشتتات السطحية على خواص العامل المساعد المحضر (SBA-15) النانوي باستخدام سليكات الصوديوم

يسرى صابر كريم [١]، حسين قاسم حسين [٢]

[١] قسم الهندسة الكيمياوية/ جامعة بغداد / بغداد – العراق.

[٢] قسم الهندسة الكيمياوية / كلية الهندسة / جامعة بغداد / بغداد – العراق.

الخلاصة

صنع العامل المساعد (SBA_15) باقطار نانوية مختلفة وخواص سطحية واشكال مختلفة بنجاح من خلال التحكم في التفاعلات المحبة والكارهه للماء (اي السيطرة على ذوبانية نويات قالب ال (p123) المستخدم في تصنيع العامل المساعد من خلال التحكم في الاشارة الواقعة في المنطقة المحصورة بين التفاعلات المحبه للماء وايونات السليكا غير العضوية تمت التجارب باستخدام ثلاث انواع من المشتتات السطحية وباشارات مختلفة وهي المشتتات الموجبة (CTAB) أو المشتتات السالبة (SBDS) أو المشتتات عديمة الشحنة (F68). تم استخدام سيلكات الصوديوم كمصدر للسيلكا في التصنيع. تم أستخدام البوليمر نوع (P123) كقالب بدرجة حامضية عالية للوسط المائي وصلت الى اقل من٢.. تم تشخيص خواص العامل المساعد بعد أجراء عدة فحوصات مثل حيود الاشعة السينية، الاشعة تحت الحمراء، برونر- أيميت- تيللير (أمتصاص وأمتزاز النتروجين)، مجهر القوة الذرية والمجهر الالكتروني الماسح. أن فحوصات حيود الاشعة السينية والاشعة تحت الحمراء اثبتت تحضير عامل مساعد ضعيف التبلور خالي من ايه شوائب. أن درجة تشتيت الدقائق للعامل المساعد المحضر كانت تتبع الترتيب CTAB>SBDS> F68> p123 . أن الخواص السطحية للعامل المساعد المحضر تتراوح بين (٥٧٧-٩٠٠) م٢/ غرام مساحة سطحية وبين (0.47-0.28) سم٣/غرام حجم فجوات وبين (2.3-1.98) نانو متر قطر فجوات. كانت النتائج المثالية المسجلة باستخدام العامل المشتت الموجب CTAB.

الكلمات الدالة: سيليكات الصوديوم، المواد المشتتة للسطوح، SBDS،CTAB .

1.INTRODUCTION

Porous materials are established as solids that have a content of pores, and the fraction of pore volume to the total volume is 0.2-0.95. These materials can be classified into (micro, meso, and macro) porous according to pore size. Due to selective size, shape, and thermal stability, microporous materials are used in limited applications concentrated on the separation of fine chemical particles [1], while mesoporous materials is more preferred for their highly ordered mesostructured, apart from high surface area, which allows diffusion and adsorption of larger molecules for wide applications than that of microstructure Due to literatures, M41S and SBA groups are the most famous ordered mesoporous materials [2-4]. The first synthesis of mesoporous material type MCM41 was attempted in 1990. This type has a high surface area with a narrow pore size, which makes it suitable for various applications, such as hosts for catalysts, drug delivery systems, and solar cells, among others. In 1998, Zhao et al. prepared a new type of mesoporous material with a uniform two-dimensional hexagonal structure, named SBA-15, using a nonionic surfactant called Pluronic 123 as a template in a highly acidic medium (pH<2). Compared to microporous MCM41, this material is characterized by a larger pore size, thicker wall, and higher thermal stability during applications [5,6]. The importance of SBA-15 comes from its applications in various fields including catalysts, petroleum refining, water treatment, sensors, and medical fields [7, 11]. In recent years, many researchers have focused on overcoming the difficulties of achieving a balance between the surface properties of prepared SBA-15, such as nanoparticle size distribution, pore size, surface area, and ordered morphology. This research is concerned with varying different conditions: pH of media [12], micelle expanders [13], dispersant agents [14], silica to surfactant ratio, silica source such as tetraethylorthosilicate (TEOS), and sodium silicate (Na_2SiO_3) [15], repining and aging temperatures [16]. Focusing on the p123 tri–block copolymer template, its role involves the formation of micelles during hydration reactions, followed by polymerization reactions with inorganic silica ions and subsequent template removal to produce mesoporous silica materials. Few researchers have attempted to use cetyltrimethylammonium bromide (CTAB) as both a co-surfactant and a main template [17]. Wesley et al. [18] investigated the morphology and texture properties of SBA-15 prepared using a ternary system of p123 as a surfactant, CTAB as a co-surfactant, and ethanol with different amounts of TEOS between 8 and 31 g as a silica source. They found that the morphology of the prepared samples was a random shape with aggregate particles at low TEOS amounts, which were converted into macrospheres 15 mm in size after using over 23 g of TEOS. Additionally, the texture properties were between 641-932 cm^2/g surface area, 0.59-0.93 cm^3/g pore volume, and 3.2-4 nm pore size [18]. Amit et al. [19] studied the effect of adding 1,3,5-trimethylbenzene (TMB) to a couple of co-surfactants of pluronic p123, besides cetyl trimethyl ammonium bromide (CTMB), for the preparation of large pore size SBA-15 used for the adsorption of biomolecules. The ratio of TMB/p123 was between 0 and 0.5 to produce spherical SBA-15 with specific texture properties of (2-12) nm pore size with high surface area, and pore volume, which reached over 700 m^2/g, and $1cm^3/g$, respectively [19]. Zainab and Sheela [20] synthesized organized mesoporous alumina using CTAB, Triton X-114, and stearic acid. They found that only CTAB surfactant produced a narrow pore size distribution of

8nm with a sufficient surface area of 280 m^2/g [20]. Altug and Omer [21] controlled the texture properties and the morphologies of synthesized mesoporous SBA-15 with and without adding different additives like; organic additives (benzene) at concentrations between 0.17-0.9M, or inorganic ones (SO_4^{-2}, NO_3^{-1}, and Cl^{-1}) at concentrations between 0.25-1 M to couple surfactants of p123, and CTAB at CTAB / P123 mole ratio between 3-6. They found that increasing the concentration of SO_4^{-2}, and benzene decreased micelle solubility, producing wormlike particles with elongated pores. However, increasing NO_3^{-1} just affects CTAB concentration in the CTAB-P123 zone, causing a drop in all texture properties. The effect of using Cl^{-1} ions is between SO_4^{-2} and NO_3^{-1} [21]. Finally, Hector et al. [22] used CTAB as a basic template for the preparation of MCM-41 mesoporous silica with CTAB/SiO_2 from 0.35 to 0.71, at aging conditions of 110 hrs., and 80 ^oC. Ordered mesoporous MCM-41 silica with optimum texture properties of 1028 m^2/g, and 1.69 cm^3/g obtained at CTAB/SiO_2 of 0.53 [22]. This paper reports a novel study on the effect of co-surfactant charge on the behavior of p123 micelles in the inorganic silica zone, and their effect on texture properties during the preparation of SBA-15.

2.EXPERIMENTAL PROGRAM

2.1.Materials

Alkaline sodium silicate with (SiO_2/ Na_2O) =1 weight ratio, prepared from previous work, was used as a silica source. Pluronic (p123) tri-block co-polymer with a MW = 5800 g/mol, (purchased from Macklin Co., Shanghai, China), was used as a template. For strong acid media during SBA-15 preparation, hydrochloric acid (HCl, 37%) from CDH was used. Cetyl trimethylammonium bromide, MW=364,45 g/mole purchased from Himedea as a cationic surfactant, sodium dodecyl benzenesulfonate, Mw= 348,48 g/mol obtained from Sigma-Aldrich as an anionic surfactant. Pluronic F68 difunctional block co-polymer with Mw= 8400 g/mole (purchased from Macklin Co., Shanghai, China), used as a nonionic surfactant, Deionized water.

2.2.Experimental Procedure

The experimental procedures are listed below:

1) Sodium silicate was prepared according to the procedure reported by Yousra and Hussein [23]. 6 g of Pluronic P123 was dissolved in 180 g of 2M HCl (solution A), and 12.75 g of the prepared sodium silicate was dissolved in 45 g of water (solution B). The two solutions were mixed under vigorous stirring (1000 rpm) in a strong acid medium (pH<2) for 24 hrs at 35^oC.
2) The mixture above was aged at 100 ^oC for 24 hrs. After aging, the solution was filtered using nano filter paper and subsequently washed with deionized water to eliminate sodium ions. The resulting powder was dried at 100 ℃ for 24 h, calcined at 550 ℃ for 6 h, and labeled (D_0).
3) The above procedure was repeated using 1 g of either CTAB, SDBS, or Pluronic F68 as co-surfactants to study their effect on the behavior of P123-inorganic silica, and their effect on the structural properties of synthesized SBA-15, which was labeled (D_1, D_2, and D_3), respectively.

2.3.Experimental Analysis and Instruments

The identification of the prepared SBA-15 was tested using a multifunctional X-ray diffractometer model Shimadzu SRD 6050, Japan, with Cu Kα radiation at 30kv and 30 mA. The tests were conducted at a 2 θ angle from 10-80^o. The surface morphology was assessed using an Inspect F50 from FEI Company in the Netherlands. The textural parameters (surface area, pore volume, and pore size) were determined using the (BET) Technique with a Thermo Analyzer, USA, at the Petroleum Research and Development Centre - Ministry of Oil, Baghdad, Iraq. The primary chemical groups of the produced SBA-15 were determined utilising a Shimadzu FT-IR-Affinity spectrometer, Japan in the transmission range of 400-4000 cm^{-1}. Finally, the nanoscale range tests were conducted using Atomic Force Microscopy (AFM) (Angstrom AA2000) at the Department of Chemistry, College of Science, Baghdad University.

3.RESULTS AND DISCUSSION

Figure 1 represents x-ray diffraction peaks of the experiments attempted at 2θ from 10 to 80^o using three different co-surfactants: cationic CTAB, anionic SDBS, and nonionic F68. This figure shows one amorphous diffraction peak located at 2θ from 20 to 25^o according to the standard (ICDD # 00-001-0424) related to the plane (100), while planes (110, and 200) do not appear when compared to the standards representing a successful synthesis of mesoporous materials with disordered SBA-15 [24]. Also, the broadening of the peaks was clearly evident due to the effect of the p123 template, which was released from the powders after calcination, producing a nanoparticle size distribution [25]. This behavior was also diagnosed by Wesley et al. [18]. When comparing the peaks obtained using p123 with those obtained using variable charge co-surfactants, there is a slight increase in 2θ diffraction angle, which corresponds to a slight increase in pore volume or pore size of samples prepared with co-surfactants. Also, the effect of adding surfactants focused on surface properties with no effect on the crystallinity of the products. This is because all the samples had been subjected to constant aging conditions of 100^{o}C, for 24 hrs, using Na_2SO_3 as

a silica source, which is easily hydrated and condensates at strong acidic conditions producing samples with low intensities and poor mesoporous properties [26, 27]. Basic chemical groups of mesoporous SBA-15 prepared from sodium silicate like Si=O, Si-O-Si, and Si-OH, without and with three different co-surfactant charges of cationic CTAB, anionic SDBS, and nonionic F68, were identified in Fig. 2 using FTIR analysis. The stretching vibration of the silanol groups (Si=O) appeared at a wavelength of around 480 cm^{-1}, while the weak vibration of the siloxane group (Si-O-Si) appeared at a wavelength of around 760 cm^{-1} [28]. The intense vibration peaks of the same chemical groups were indicated over 1100 cm^{-1} [29]. The peaks in 2900 cm $^{-1}$ indicate the formation of Si–OH groups. There are no broad bands behind the region of 3400cm^{-1} because of the absence of –OH groups in all prepared samples [30]. Particle size distribution, 3-D topographic shapes, and the texture properties of prepared samples without and with three different charge co-surfactants are shown in Figs. 3-6 and listed in Table 1. The nanoscale particle sizes are between (32-70) nm, while the texture properties are between (577-900) m^2/g Surface area, (0.28-0.47) cm^3/g pore volume, and almost 2 nm pore size for all experiments.

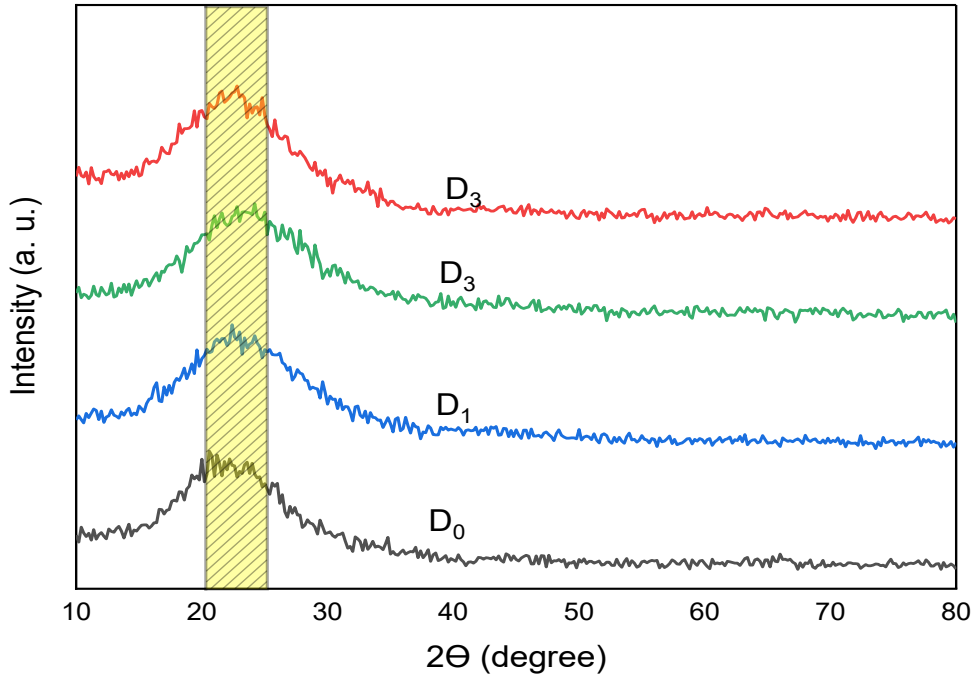

Fig. 1 X-ray Diffraction of Prepared SBA-15 Using p123 (D_0), p1213+CTAB (D_1), p123+SDBS (D_2), and p123+F68 (D_3).

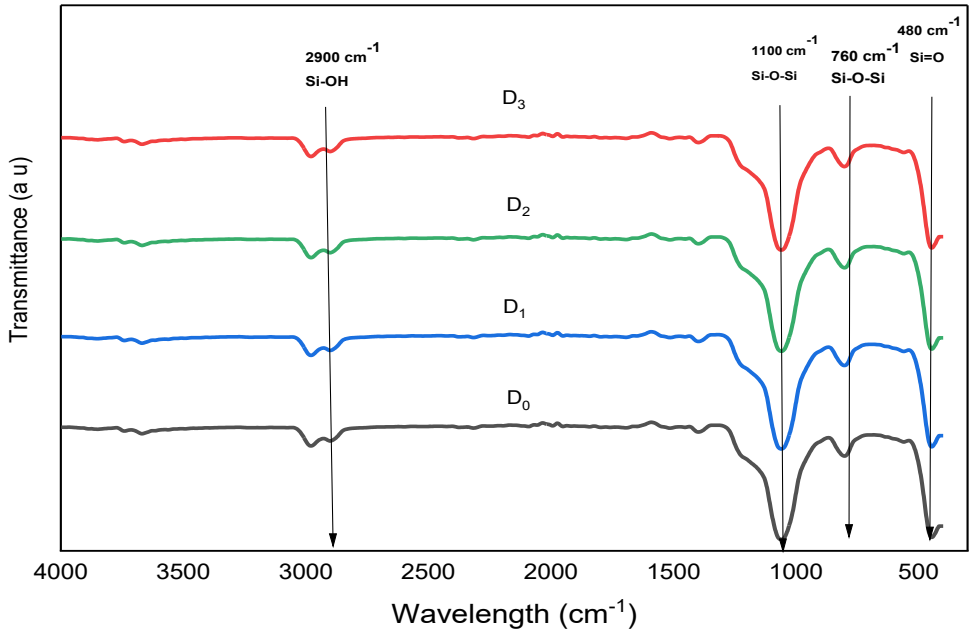

Fig. 2 FTIR of Prepared SBA-15 Using p123 (D_0), p1213+CTAB (D_1), p123+SDBS (D_2), and p123+F68 (D_3).

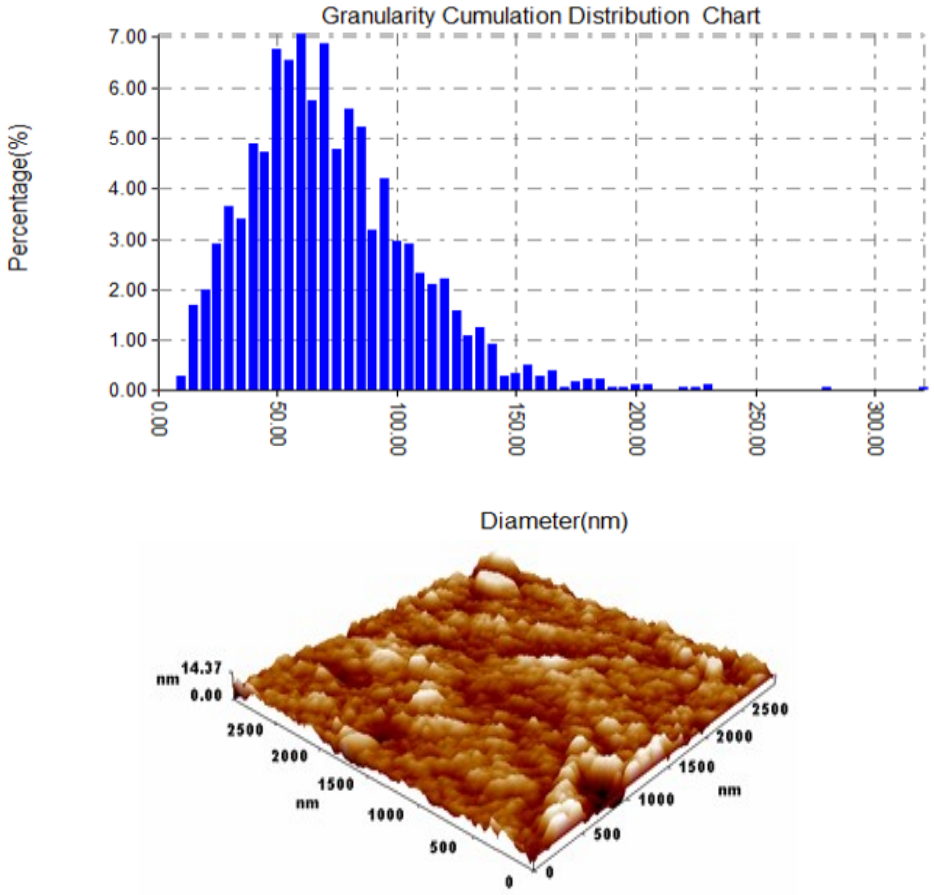

Fig. 3 Particle Size Distribution and 3D Images in Topography for Prepared SBA-15 Using Bare p123 (D_o).

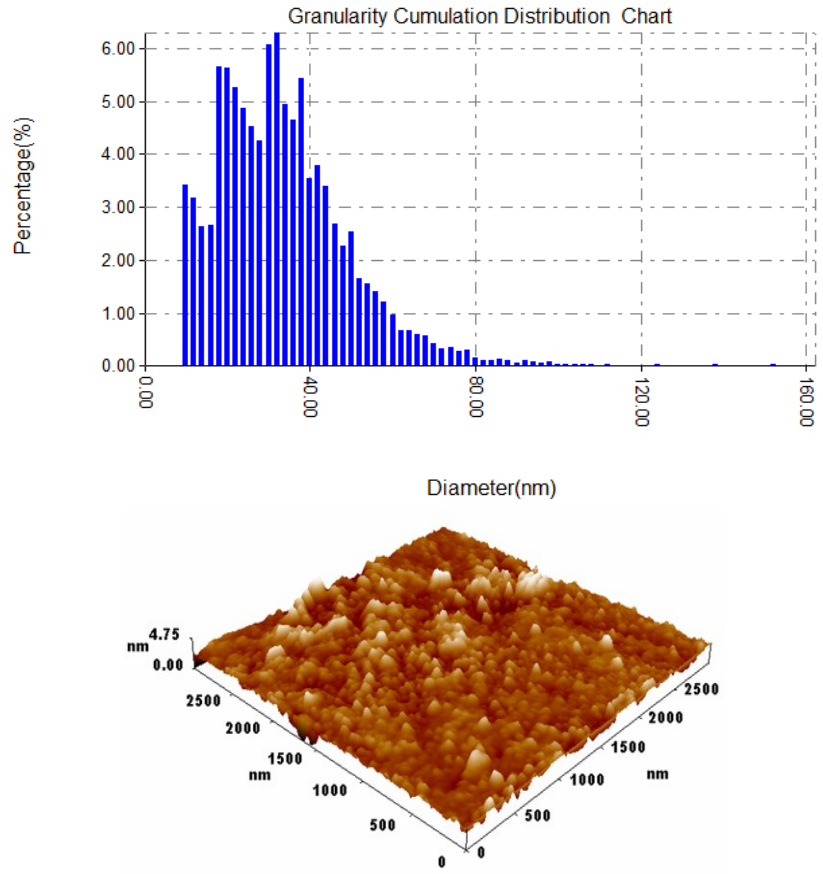

Fig. 4 Particle Size Distribution and 3D Images in Topography for Prepared SBA-15 Using p123 + CTAB (D1).

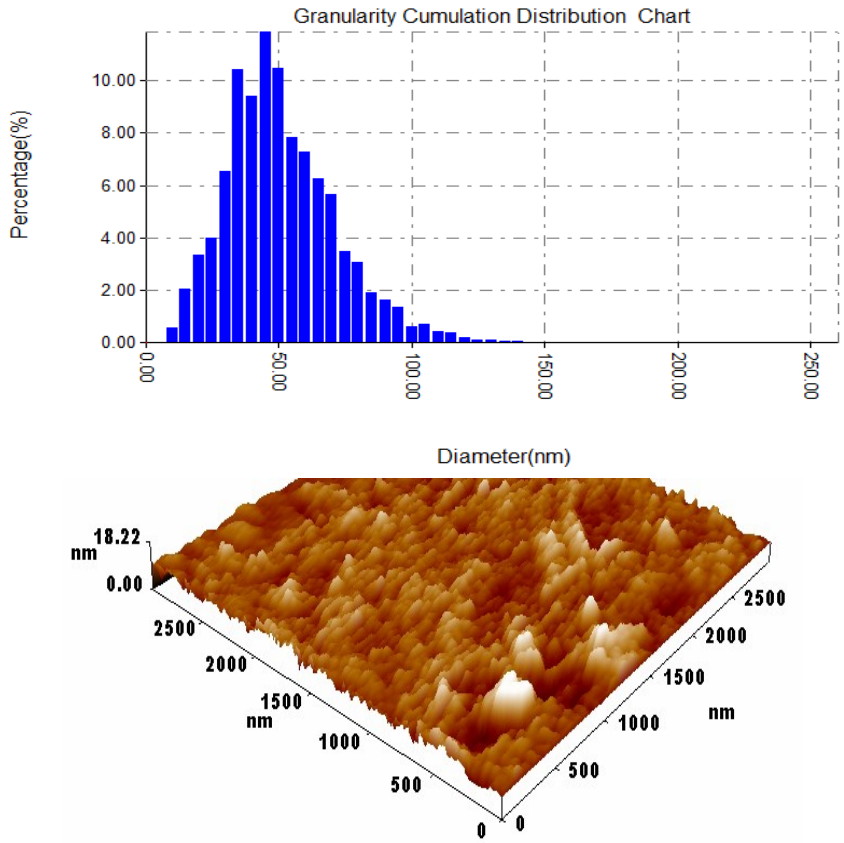

Fig. 5 Particle Size Distribution and 3D Images in Topography for Prepared SBA-15 Using p123 + SBDS (D_2).

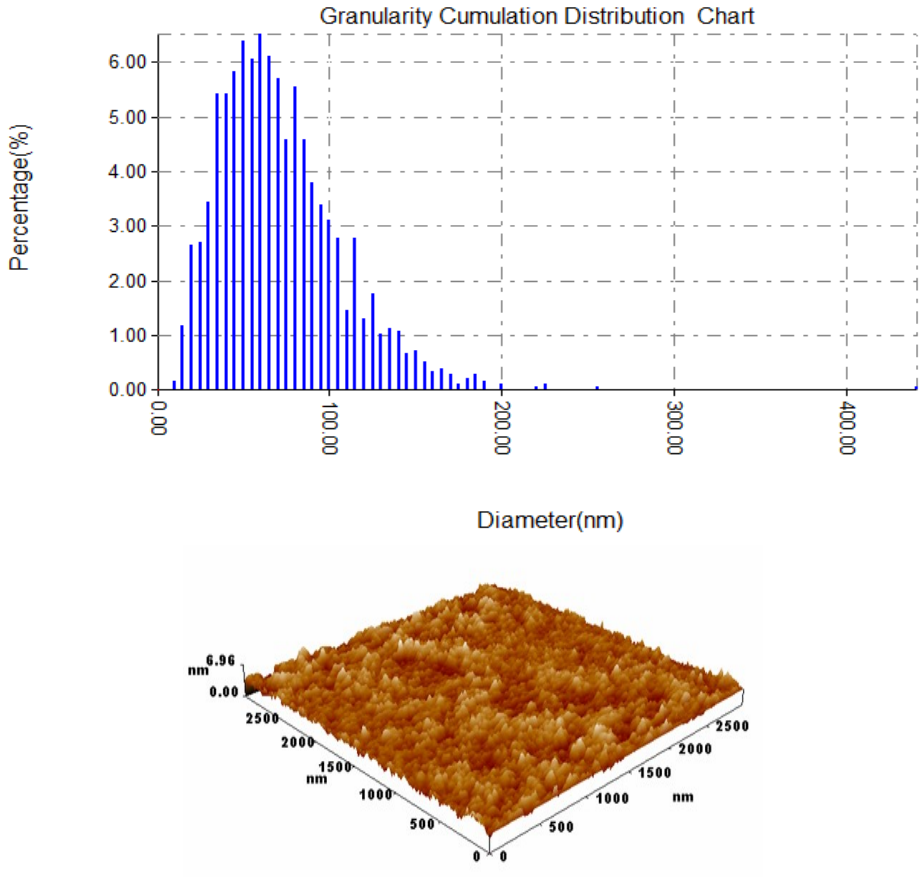

Fig. 6 Particle Size Distribution and 3D Images in Topography for Prepared SBA-15 Using p123 + SBDS (D_3).

Table 1 Average Particle Size and Texture Properties Results of Prepared Samples.

Experiment code	Av. P. size (nm)	S.A. (m^2/g)	P. V.(cm^3/g)	P. S. (nm)
D_0, p123	69.9	577	0.28	1.98
D_1, p123 + CTAB	32.7	900	0.47	2.1
D_2, p123 + SDBS	49.1	769	0.43	2.3
D_3, p123, + F68	69.4	647	0.37	2.3

The dispersion of mesoporous SBA-15 particles, and their texture properties are sufficiently related to the hydration–dehydration reactions that happened in p123 micelles – inorganic silica zone. These reactions are pH- and temperature-dependent. Besides the synthesis of SBA-15, using sodium silicate as a silica source without any co-surfactants at strong acid media causes rapid polymerization (condensation) between the PEO chain in p123 micelles in silica ions [31, 32]. Beginning of bare p123 micelles, the reaction happened rapidly at the micelles wall, which represents a template of mesoporous materials in mild aging conditions of 100˚C, and a short period of 24 hrs. (D_0), producing a weak dispersion of particles reaching 70 nm with a surface area of 577 m^2/g, and low mesoporous properties. According to the literature, it was reported that in the absence of any co-surfactants, the interaction between PEO-PPO chains of P123 micelles (S^0) with anionic silica ions acting from sodium silicate (X-) happened in an acidic medium (I^+) according to the ionic pair of ($S^0 I^+ X^-$). This interaction is sufficiently affected by any additives, such as solvents, inorganic salts, micelle expanders, and variable surfactants [18]. The effect of three co-surfactants added in this work depends on their head group charge. Firstly, using cationic CTAB as a co-surfactant in SBA-15 synthesis increases H^+ ions in PEO-silica ions according to the ionic pair of ($S^0H^+X^-I^+$), so that the hydration, and condensation reactions are reached to its optimum values causes highly dispersion of particles reached to 32nm, which producing optimum texture properties of $900 m^2/g$ surface area, 0.47 cm^3/g pore volume, with no effect on the pore size of 2nm. In comparison with other research using CTAB as a co-surfactant, and TEOS as a silica source, the recorded texture properties were between (700-900) m^2/g surface area, (0.5-0.9) cm^3/g pore volume, and 12-15nm pore size after adding the ethanol as a co-solvent, and trimethylbenzene (TMB) as micelles expanders, respectively [18, 19]. On the other hand, using SDBS as an anionic co-surfactant in SBA-15 synthesis has two variable effects in the two hydration reaction zones. In the P123 hydration reactions zone SBDS has an opposite charge to enhance these reactions, however, it has a negligible effect on decreasing the solubility i.e. increasing micellization of P123 micelles, while in the inorganic silica, hydration zone using SBDS gives an abundance of negative ionic charges ready to hydrate, and polymerized in moderate aging conditions producing moderate dispersion of particles reached to 49nm, and sufficient texture properties of $770 m^2/g$ surface area, 0.43 cm^3/g pore volume with almost constant 2nm pore size. This behavior is similar to that recorded by Altug and Omer [21]. Using F68 as a nonionic surfactant in SBA-15 synthesis can disperse particles lower than the other two surfactants used, resulting in a 69nm average particle size, with lower texture properties of 647 m^2/g surface area, and 0.37 cm^3/g pore volume and a nearly constant 2nm pore size. Their effect focused on the weak but sufficient interaction between the lonely PEO chain in its structure and the other one in P123 increasing the vacancies (size) of hydrophilic zones ready to hydrate, and condensate during SBA-15 synthesis. Finally, the three-dimensional surface morphology using the bare p123 template, and p123+CTAB represents a semi-spherical shape and this shape deforms after using SBDS and F68 surfactants. This morphology matches that of the other one attempted using FESEM techniques.

Table 2 Texture Properties Results of previous Work.

Author name	variables	S.A. (m^2/g)	P. V. (cm^3/g)	P. S. (nm)
Wesley et al. [18]	P123, CTAB, ethanol	641-932	0.59-0.93	3-4
Amit et al. [19]	P123, CTAB, TMB micelle expander	700-900	1.04-1.64	12-15
Altug and Omar [21]	P123, CTAB, SO_4^{-2}, Benzen	528-723	0.4-0.96	2.5-7
Present Work	P123+CTAB, or p123+F68, or p123+ SDBS	577-900	0.28-0.47	1.98-2.3

According to works of literature, SBA-15 has variable morphologies including spheres, rod-like, fibrous, donuts, gyroids, ropes, and others. Surface morphologies of prepared SBA-15 samples without and with three variable charge co-surfactants, magnified by 13000 times, are shown in Fig. 7. The morphology of the SBA-15 sample synthesized without co-surfactant (using bare p123 template), named as D_0, has a semi-spherical shape, and this surface shape matches the morphology shown by Sara et al. [33]. Using CTAB as a co-surfactant in sample D_1 controls the surface morphology of particles to a more regular spherical shape with a smaller particle size compared to D_0. This behavior occurred because the positive head group charge of CTAB is curved micelles' wall during highly hydration-condensation reactions before

the dispersion role of this surfactant. A similar morphology was reported by Amit et al. [19], while an aggregate random shape was diagnosed by Wesley et al. [18]. On the other hand, using SBDS as an anionic co-surfactant produces rod-like shape. This morphology is due to the dual functions of SBDS between the PEO-PPO zone and ionic silica zone, as stated above, which leads to a transfer in morphology from a semi-spherical shape to a rod-like one. This behavior is similar to that recorded by Altug and Omer using variable additives of SO_4^{-2} ions and benzene [21]. Finally, the use of F68 as a non-ionic co-surfactant causes deformation to an irregular shape, because of its PEO role, which reacts with PEO chain in p123 micelles changing the path of hydration-condensation reactions effecting the final structure, with slight dispersion in particles.

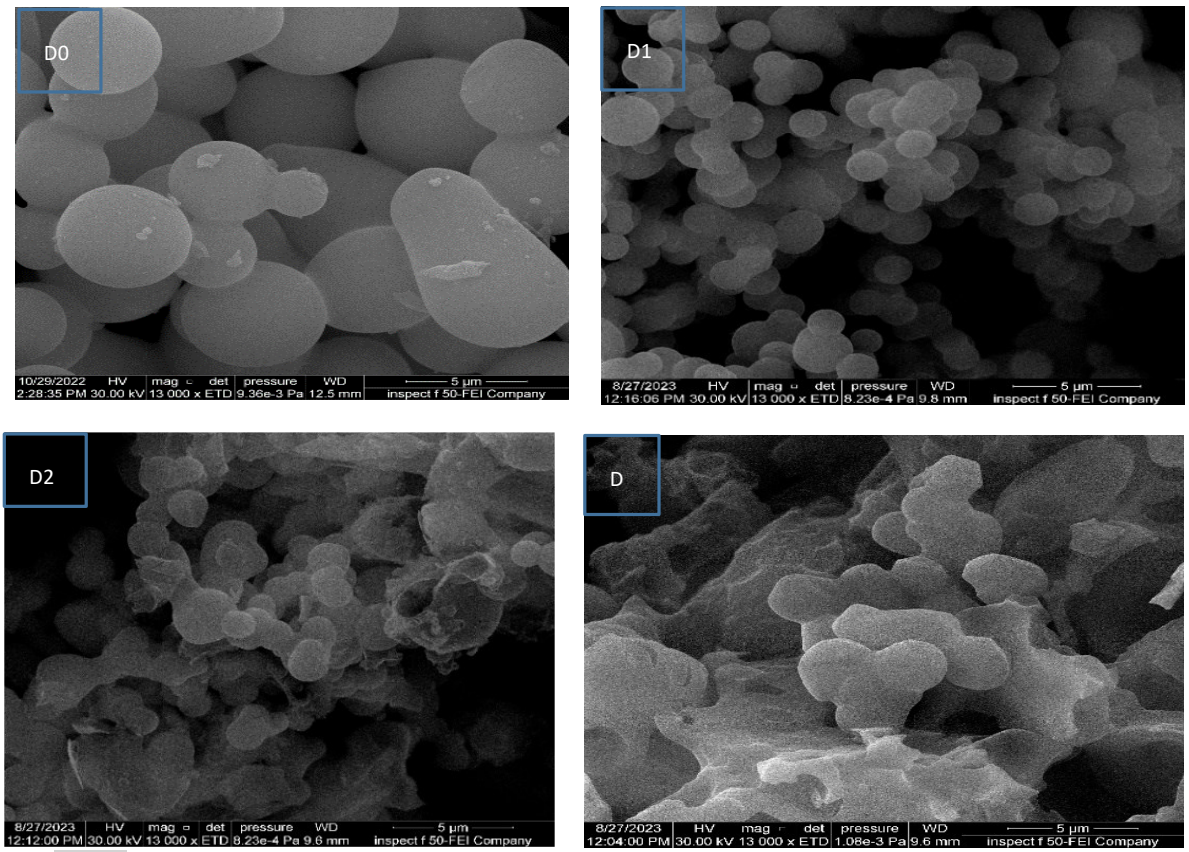

Fig. 7 FESEM of Prepared SBA-15 Using p123 (D_0), p1213+CTAB (D_1), p123+SDBS (D_2), and p123+F68 (D_3).

4.CONCLUSIONS

The present work shows an effective synthesis of mesoporous SBA-15 nanoparticles (MSN) without, and with three variable charges of co-surfactants using prepared sodium silicate as a silica source under moderate hydrothermal conditions. It is clear from the estimated texture properties that the role of the charge of co-surfactants added during SBA-15 synthesis primarily affects the surface area, with a minor effect on pore volume, while the pore size of samples did not surpass a magnitude of 2 nanometers. This behavior occurred due to using variable co-surfactants, which increased the hydrolysis reactions between the PEO hydrophilic chains of P123 micelles and inorganic silica ions, without opposite dehydration reactions associated with the hydrophobic zone of P123 micelles. Additionally, all experiments were conducted at fixed thermal conditions (100°C, 24 hrs.), which is insufficient for the dehydration reactions using sodium silicate as a silica source, as these reactions require at least 3 days to accumulate the hydration-dehydration equilibrium. The optimum texture properties of 32nm average particle size, 900m^2/g, 0.47 cm^3/g, and 2nm pore size were obtained using 1g CTAB positive co-surfactant. The prepared SBA-15 with high surface area and low mesoporous properties is suitable for many applications, such as catalysts, adsorbents, drug delivery, and others. The future scope of work will focus on studying the effect of using a combination of additives, such as surfactants and swelling agents, with sodium silicate to produce SBA-15 with highly mesoporous properties, characterized by a long crystallization time.

ACKNOWLEDGMENTS

The authors are grateful for the financial support towards this research by the Chemical Engineering Department, College of Engineering, Baghdad University.

Postgraduate Research Grant (PGRG) No.45/2637/in 28/10/2020.

REFERENCES

[1] Maha NI, Ghassan HA, Hatem M, Fatin HY. **MnO2 Nano Particles Modified a Double Layer Cathode Reactor for an Efficient Removal of DBT in Diesel**. *Tikrit Journal of Engineering Sciences* 2024; **31**(3): 44-59.

[2] Ayser J, Hamin JM. **Experimental Design of Oxidative Desulfurization of Kerosene Through Response Surface Methodology (RSM)**. *Tikrit Journal of Engineering Sciences* 2023; **30**(2): 130-141.

[3] Norhasyimi R, Ahmad ZA, Abdullah RM. **A Review: Mesoporous Santa Barbara Amorphous-15, Types, Synthesis and Its Applications towards Biorefinery Production**. *Journal of Applied Sciences* 2010; **7**(12): 1579-1586.

[4] Shakir F, Hussein QH, Zeinab TA. **Preparation and Characterization of High Surface Area Nanosilica from Iraqi Sand via Sol-Gel Technique**. *Journal of Petroleum Research and Studies* 2022; **12**(4): 104-117.

[5] Sama MA, Serhan IA, Stuart MH. **Using the Ash of Common Water Reeds as a Silica Source for Producing High Purity ZSM-5 Zeolite Microspheres**. *Microporous and Mesoporous Materials* 2021; **316**: 110953.

[6] Shizaki K, Komarneni S, Nanko M. **Porous Materials: Process Technology and Applications**. Materials Technology Series 4, Springer US; 1998.

[7] Wesley JJ, Stevens EA. **Investigation of the Morphology of the Mesoporous SBA-16 and SBA-15 Materials**. *Journal of Physical Chemistry* 2006; **110**(18): 9183-9187.

[8] Kaiyu BA, Junsheng HA, Yongxing YA, Aniu QB. **The Effect of Hydrothermal Temperature on the Properties of SBA-15**. *Heliyon* 2020; **6**(6): e04361.

[9] Nisreen SA, Ziad TA, Hasan SM, Maher AA, Saady NMC, Talib MA. **Modification of SBA-15 Mesoporous Silica as an Active Heterogeneous Catalyst for Hydroisomerization of n-Heptane**. *Heliyon* 2022; **8**(6): e09745.

[10] Talib MA, Doyle AM. **SBA-15 Supported Bimetallic Catalysts for Enhancement Isomers Production During n-Heptane Decomposition**. *International Journal of Chemical Reactor Engineering* 2014; **12**(1): 1-10.

[11] Mohammed AA, Hussain HS, Abdullah SK. **Use of Zeolite to Reduce the Activity of Cesium-137 in the Liquid Waste**. *Iraqi Journal of Physics* 2021; **19**(49): 1-6.

[12] Lashgari N, Badiei A, Ziarani GM. **A Novel Functionalized Nanoporous SBA-15 as a Selective Fluorescent Sensor for the Detection of Multianalytes (Fe3+ and Cr2O72-) in Water**. *Journal of Physical Chemistry* 2017; **121**(19): 238-248.

[13] Tomer VK, Devi S, Malik R, Nehra SP, Duhan S. **Fast Response with High-Performance Humidity Sensing of Ag–SnO2/SBA-15 Nanohybrid Sensors**. *Microporous and Mesoporous Materials* 2016; **219**: 240-248.

[14] Made JR, Camellia P. **Synthesis of Silica Particles by Precipitation Method of Sodium Silicate: Effect of Temperature, pH and Mixing Technique**. *AIP Conference Proceedings* 2020; **2219**(1): 080018.

[15] Michal K, Liang C. **Pore Size Tailoring in Large-Pore SBA-15 Silica Synthesized in the Presence of Hexane**. *Langmuir* 2007; **23**(13): 7247-7254.

[16] Wang W, Wu Ch, Sun R, Li D. **Simple and Controllable Preparation of SBA-15 Microspheres by Poly (Vinyl Alcohol)-Assisted P123 Templating System**. *Microporous and Mesoporous Materials* 2020; **302**: 110200.

[17] Ahmad ZA, Razali N, Keat-Teong L. **Influence of the Silica-to-Surfactant Ratio and the pH of Synthesis on the Characteristics of Mesoporous SBA-15**. *Journal of Physical Science* 2010; **21**(2): 13-27.

[18] Ridhawati T, Abdul Wahid W, Nursiah LN. **Synthesis of High Surface Area Mesoporous Silica SBA-15 by Adjusting Hydrothermal Treatment Time and the Amount of Polyvinyl Alcohol**. *Open Chemistry* 2019; **17**(1): 963-971.

[19] Yong W, Yinjie Z, Jun Ch, Zheng L, Haiqing W, Qinglin S, Bing H, Yan K. **Synthesis, Characterization and Catalytic Activity of Binary Metallic Titanium and Iron-Containing Mesoporous Silica**. *Microporous and Mesoporous Materials* 2012; **162**: 51-59.

[20] Wesley JJ, Kurt L, Gustaaf VT. **Investigation of the Morphology of the Mesoporous SBA-16 and SBA-15 Materials**. *Journal of Physical Chemistry* 2006; **110**(18): 9183-9187.

[21] Amit K, Santosh Y, Panagiotis GS. **Synthesis of Ordered Large Pore SBA-15 Spherical Particles for Adsorption of Biomolecules**. *Journal of Chromatography* 2006; **1122**(1-2): 13-20.

[22] Ramli R, Sheela Ch. **Effect of Templates on the Synthesis of Organized Mesoporous Alumina**. *Malaysian Journal of Analytical Science* 2007; **11**(1): 110-116.

[23] Altug SP, Omer D. **Role of Organic and Inorganic Additives on the Assembly of CTAB-P123 and the Morphology of Mesoporous Silica Particles**. *Journal of Physical Chemistry* 2009; **113**(43): 18596-18607.

[24] Héctor I, Meléndez-O M, Alfonso MS, Luis AG. **Hydrothermal Synthesis of Mesoporous Silica MCM-41 Using Commercial Sodium Silicate**. *Journal of Mexican Chemical Society* 2013; **57**(2): 73-79.

[25] Yousra S, Hussein QH. **Synthesis and Characterization of Sodium Silicate from Iraqi Silica Sand: Effect of NaOH/Sand Ratio and Fusion Temperature**. *Kongzhi yu Juece/Control and Decision* 2023; **38**(5): 1-14.

[26] Brunauer S, Deming L, Deming W. **On the Theory of the van der Waals Adsorption of Gases**. *Journal of the American Chemical Society* 1940; **62**(7): 1723-1732.

[27] Sofia M, Carlos M, Joaquin P. **Short Channel Mesoporous SBA-15 Silica Modified by Aluminum Grafting as a Support for CoRu Fischer-Tropsch Synthesis Catalyst**. *Catalysis Science and Technology* 2021; **12**(13): 4245-4258.

[28] Amanda MM, Juliusz W, Albert SJ. **Investigation of Structural Order and Morphology of MCM-41 Mesoporous Silica Using an Experimental Design Methodology**. *Journal of Porous Materials* 2006; **13**(1): 37-47.

[29] Haresh MM, Kannan S, Bajaj HC, Manu V, Raksh VJ. **A Simple Room Temperature Synthesis of MCM-41 with Enhanced Thermal and Hydrothermal Stability**. *Journal of Porous Materials* 2008; **15**(5): 571-579.

[30] Norhasyimi R, Fazlena H, Norsuraya S, Marissa M, Muhammad MZ. **Sodium Silicate as a Source of Silica for Synthesis of Mesoporous SBA-15**. *IOP Conference Series: Materials Science and Engineering* 2016; **133**(1): 012011.

[31] Erdem B, Erdem S, Mustafa RÖ. **Catalytic Applications of Large Pore Sulfonic Acid-Functionalized SBA-15 Mesoporous Silica for Esterification**. *Open Chemistry* 2018; **16**(1): 1233-1241.

[32] Dong Y, Lu B, Zang Sh, Zhao J, Wang X, Cai Q. **Removal of Methylene Blue from Colored Effluents by Adsorption onto SBA-15**. *Journal of Chemical Technology and Biotechnology* 2010; **86**(4): 216-219.

[33] Kim SS, Karkamkar A, Pinnavaia TJ, Kruk M, Jaroniec M. **Synthesis and Characterization of Ordered, Very Large Pore MSU-H Silicas Assembled from Water-Soluble Silicates**. *Journal of Physical Chemistry* 2001; **105**(32): 7663-7670.

[34] Berggren A, Palmqvist AEC. **Silica-Based Mesoporous Nanoparticles for Controlled Drug Delivery**. *Journal of Physical Chemistry* 2008; **112**(4): 732-737.

[35] Sara FHT. **Effects of Synthesis Conditions on the Textural and Morphological Properties of Mesoporous Silica (SBA-15)**. *Applied Mechanics and Materials* 2014; **446-447**: 201-205.